CHARACTERIZATION OF MULTI-WALLED CARBON NANOTUBES ACTIVATED BY KOH

Yong Chen, Chang Liu, Hui-Ming Cheng*
Shenyang National Laboratory for Materials Science, Institute of Metal Research,
Chinese Academy of Sciences, 72 Wenhua Road, Shenyang 110016, P. R. China

Corresponding author e-mail address: cheng@imr.ac.cn

Introduction

Carbon nanotubes (CNTs) are expected to have potential applications as composite reinforcement, catalyst support, field emitters, hydrogen storage media [1, 2] and super- capacitor electrodes etc,because of their special characteristics, such as one-dimensional nano-scale hollow core, high surface area with a narrow pore distribution, and good chemical stability. In particular, high specific surface area is highly demanded in such applications as gas adsorption and super-capacitor electrode. The theoretical surface area of CNTs is very high, 2600 m2/g for SWNTs with opened ends. However, as-prepared CNTs are usually entangled with one another and have closed caps, so their specific surface area is quite low (~100 m2/g). Some efforts, such as cutting and opening the end of MWNTs [3], or using chemical treatment to create micropores on the wall of MWNTs, have been made to increase the specific surface area. KOH are usually used as activation agent to prepare activated carbon with high specific surface area [4, 5], and Jiang et al. [6] reported that MWNTs mixed with KOH by an agate mortar followed by high temperature treatment had a specific surface area of 510.5 m2/g. Because the as-prepared MWNTs are long and entangled this method was not so effective in dispersing MWNTs with solid KOH. On the other hand, the close ends of MWNTs prohibited KOH from entering the core of MWNTs.It was reported that ball milling was very effective in opening the end of MWNTs and cutting MWNTs [7, 8, 9], and also very effective in uniformly mixing different materials. Therefore, ball milling may be more efficient for changing the surface characteristics of a material.

In this paper, multi-walled carbon nanotubes (MWNTs) were purified, ball milled with KOH, and activated at high temperature. The specific surface area of the MWNTs was improved by a factor of 12.0 after the KOH activation, and a high value of 785.2 m2/g was achieved. The microstructure of the activated MWNTs was characterized by laser Raman and cryo-nitrogen adsorption. The adsorption isotherms were analyzed by adsorption potential distributions (APDs), and the working mechanism of KOH activation was also discussed.

Experimental

The MWNTs used in our experiments were prepared by a floating catalyst method [10]. Before the KOH activation, the as-prepared MWNTs were purified by air oxidation to remove amorphous carbon. The ball milling of the MWNTs and KOH mixture was performed in a stainless steel vessel under 0.8 MPa hydrogen gas atmosphere. The milled mixture was heated to 1123 K and held for 1 h under argon flow in a horizontal furnace. Then the sample was washed by concentric hydrochloric acid and de-ionized water. Finally, the activated MWNT sample was treated at 1173 K for 1 h under argon atmosphere to remove possible adsorbed gases and oxygen containing functional groups. Part of the obtained sample was graphitized for 1 h at 3073 K for comparison.

The pore structures of the as-prepared, purified, activated and graphitized MWNTs were analyzed by nitrogen adsorption measurements at 77.35 K. Before the measurements, all the samples were degassed in vacuum at 473 K for 9h. Laser Raman measurements were employed for checking the structure change caused by the activation.

Results and discussion

From TEM image as shown Fig.1, we can see that the purified MWNTs with diameters of 20-40 nm are long, straight, and in high purity (Fig. 1(a)). After ball
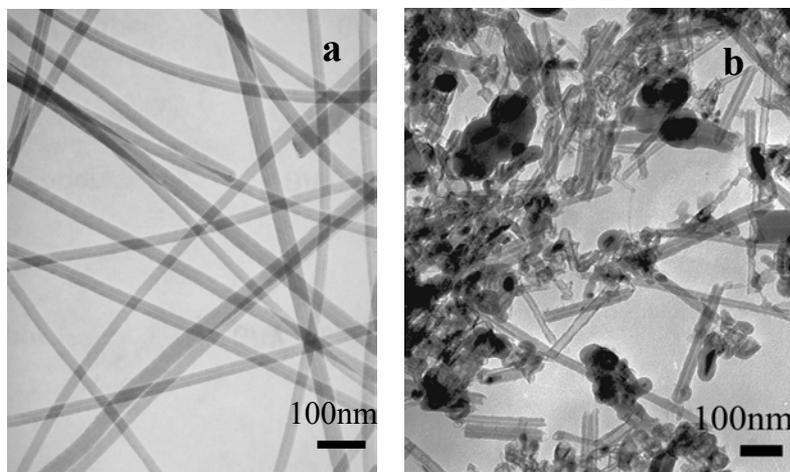

Fig. 1. TEM images of MWNTs before (a) and after (b) activation

milling and activation by KOH, it can be see that the MWNTs turned much shorter, and their inner hollow core became much larger, possibly caused by KOH etching effect (Fig. 1(b)). During the ball milling process, frequent collision and friction between balls and MWNTs made the MWNTs short cut and caused many defects on the wall of MWNTs. At the same time , the ball milling process uniformly dispersed KOH onto MWNTs, which was very important for uniform activation of MWNTs.

Fig. 2 shows the nitrogen adsorption isotherms of the MWNTs in different states. Pronounced initial increase of the adsorbed nitrogen amount for the activated MWNTs was observed below P/P0 = 0.05, suggesting the presence of abundant
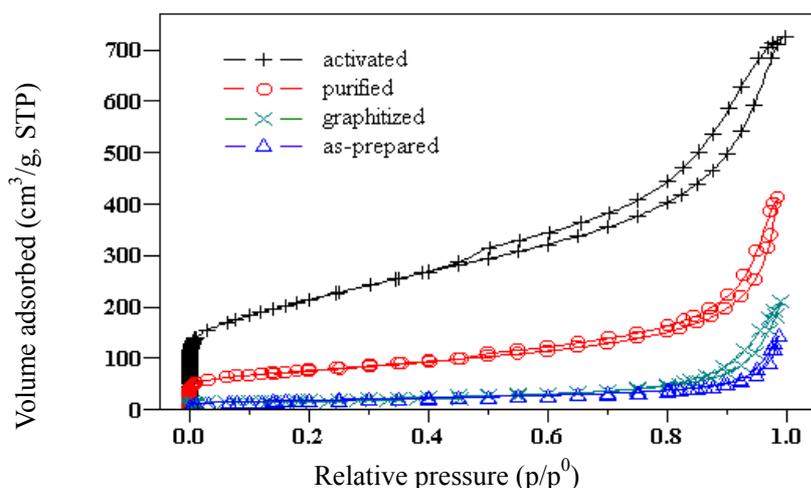

Fig. 2. Cryo-nitrogen adsorption isotherms of MWNTs

micropores and strong interaction between nitrogen molecules and the MWNTs. On the other hand, a gradual uptake of N_2 was observed at the medium P/P0, which shows adsorption of N_2 on the external surface of the activated MWNTs. The appearance of clear hysteresis indicates that many mesopores were generated by the KOH activation. Whereas the isotherms of the as-prepared and graphitized MWNTs showed no obvious increased adsorption below P/P0 = 0.05, nor at medium P/P0, due to their low micropore volume and small external surface. The hysteresis loop of the graphitized MWNTs turned much smaller, because the mesopores on the MWNT wall may be removed during the high temperature treatment at 3073 K. The comparison of specific surface area and pore structural parameters of the MWNTs in different states is given in Table 1. The BET specific surface area of the as-prepared MWNTs was 65.7 m2/g and that of activated MWNTs was 785.2 m2/g, about 12 times higher. The micropore volume of the non-activated MWNTs was 0.0088 cm3/g, but that of activated MWNTs increased to 0.1654 cm3/g. The specific surface area of the activated MWNTs dropped sharply to 61.0 m2/g after the graphitization treatment, since most micropores of MWNTs were removed to form intact graphitic sheets. Thus, it may be reasonable to believe that the micropores are created mainly in the wall of MWNTs.

Table.1 The parameters of pore structure of MWNTs in different states

Sample	SBET(m2/g)	Vmi (cm3/g)	Vme(cm3/g)
As-prepared	65.7	0.0088	0.1182
Purified	270.4	0.0557	0.5546
Activated	785.2	0.1654	1.0438
Graphitized	61.0	0.0169	0.2334

S_{BET} –BET specific surface area V_{mi}-micropore volume
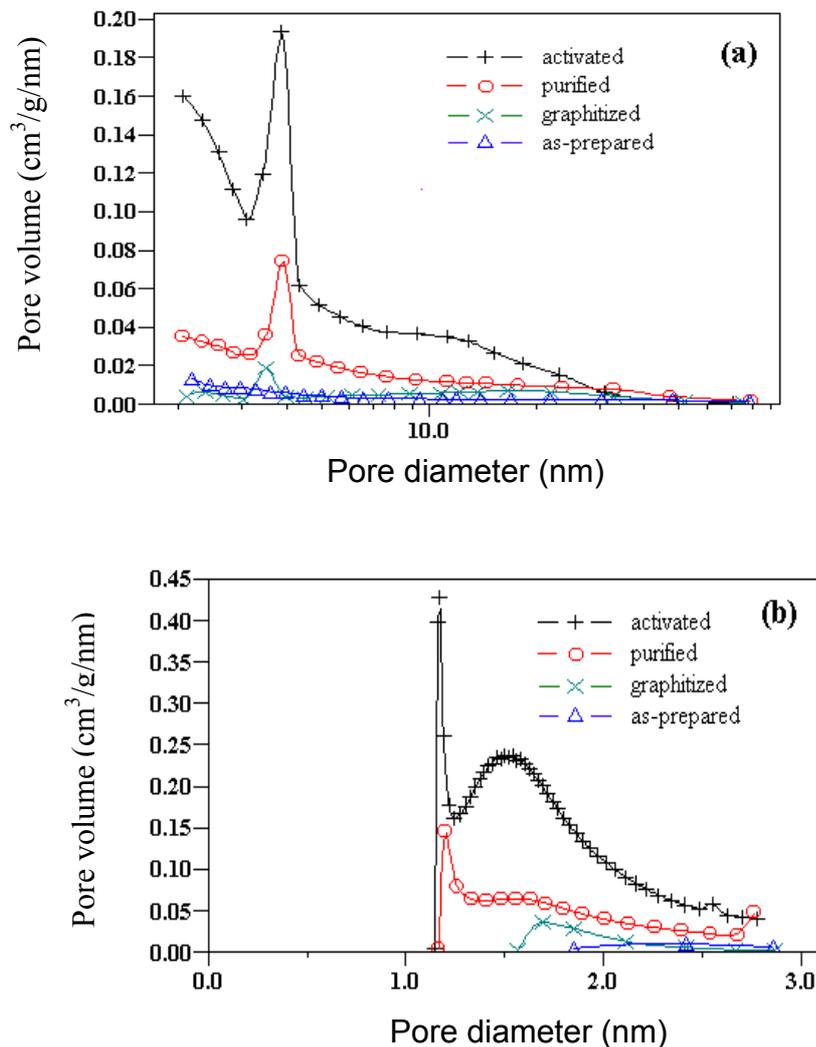
V_{me}-the mesopore volume

Fig. 3. The pore size distribution of MWNTs. (a) medium pores abtained
from BJH equation and (b) micropores abtained from HK equation

The mesopore structure elucidated from BJH equation and micropore structure from
HK equation are shown in Fig. 3. The MWNTs show only one pore distribution peak in
the range of 3 to 4 nm, except for the as-prepared sample (Fig. 3 (a)). Because the
inner core can not disappear during graphitization, the pore volume of the graphitized
MWNTs in the range of 3-4 nm and 1.5-2 nm come from the inner tubes. Part of pores
of activated MWNTs,in a diameter of 3-4 nm are attributed to the core of MWNTs and
activated mesopores. Two pore volume peaks at 1.25 nm and 1.5 nm are observed in
Fig. 3 (b). The micropores about 1.5 nm are attributed to the small core of MWNTs
and activated pores. The as-prepared and graphitized MWNTs have no pores with
diameter of 1.25 nm,which indicates that these pores were produced by oxygen
oxidization and KOH activation. From Fig. 3, we can see that the pore volume of
mesopores and micropores in MWNTs greatly increased by KOH activation.

The adsorption potential distributions (APDs) give information on the interaction

between absorbed nitrogen molecules and pore walls [11]. APD function $X(A)$ is defined as $X(A)=-d(V)/dA$, where $d(V)$ denotes the volume of adsorbed liquid nitrogen (in cm^3) per gram carbon as a function of the adsorption potential A, and A is defined as the negative change of the Gibbs free energy ΔG of adsorption, i.e. $A=-\Delta G=RT\ln(p_0/p)$. The symbols p, p_0, T and R denote, respectively, the equilibrium pressure, saturation vapor pressure, absolute temperature and universal gas constant.

The APDs of different treated MWNTs are shown in Fig. 4. All the adsorption potential of the as-prepared MWNTs was smaller than 3.5 kJ/mol because of the low content of micropores. The adsorption potential of the graphitized MWNTs was smaller than 5.5 kJ/mol, but showed two peaks, at 0-3 kJ/mol and 3-5.5 kJ/mol, respectively, due to the existence of a small amount of mesopores. The adsorption potential of the purified and activated MWNTs had three peaks: 0-3 kJ/mol, 3-8 kJ/mol and 8-8.8 kJ/mol, respectively, but the peak intensity of the activated MWNTs was much stronger than that of the purified MWNTs. The high adsorption potential between 8-8.8 kJ/mol corresponds to micropore filling in small micropores, while the peak between 3-8 kJ/mol can be attributed mostly to the monolayer formation in larger micropores or mesopores. The peaks around 0.5-3 kJ/mol possibly resulted from the multilayer adsorption in mesopores. From fig.4 So we can have the conclusion that in the KOH-activated MWNTs, the stronger peak between 3-8 kJ/mol indicates plenty of mesopores increased, and the stronger peak between 8-8.8 kJ/mol shows lots of micropores existed.
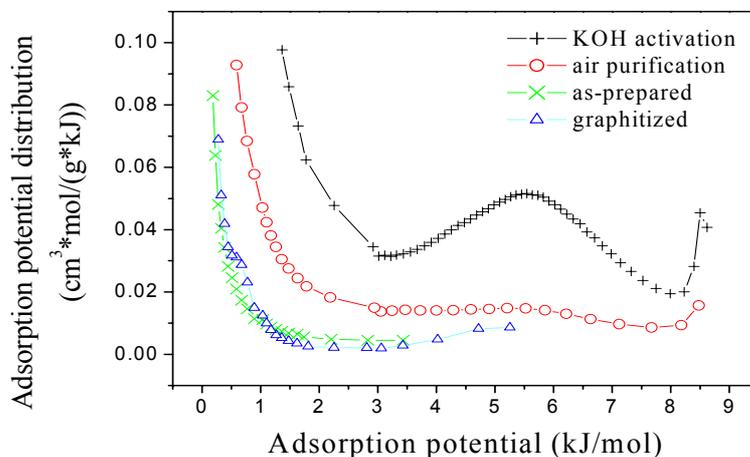
Laser   Raman

Fig. 4. Adsorption potential distributions of MWNTs

measurement is an effective method to characterize the structure of carbon materials. The laser Raman spectra of the different MWNT samples are shown in Fig. 5. The peak at around 1326 cm^{-1} can be assigned to be "D-band", which is caused by induced defects or disorder of the carbon material. The peak at 1582 cm^{-1}, so-called "G band", is assigned to the in-plane displacement of carbon atoms in hexagonal sheets. Comparing the spectrum of activated MWNTs to that ofpurified MWNTs, no

obvious difference was found, except for the intensity ratio of the D band to G band (I_D/I_G). It is generally agreed that the I_D/I_G ratio provides a useful index for comparing the crystallite sizes and disorder degree of various carbon materials. Since I_D/I_G increased from 1.06 to 1.29, it can be inferred that the crystallite size of the MWNTs decreased after activation, caused by mechanical ball milling and KOH chemical etching. However, the ID/IG decreased from 1.29 to 0.5 after graphitization, indicating
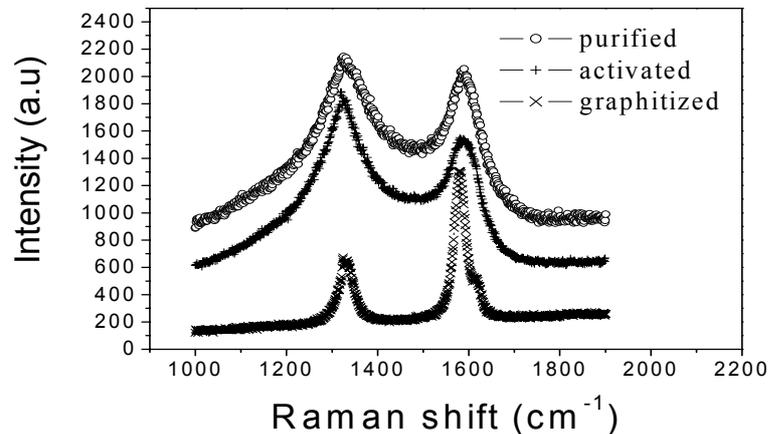

Fig. 5. Laser Raman spectra of the MWNTs before activation,
after activation and after graphitization

that the crystallite size became larger, and the defects were cured by the high temperature treatment.

Conclusions

MWNTs with a high specific surface area of 785 m2/g were obtained by activation using KOH at 1173 K. The MWNTs were short cut and the crystalline size turned smaller after activation. Abundant mesopores and micropores were developed in the activated samples. Most micropores and defects of the activated MWNTs can be removed by high temperature graphitization, which also results in a sharp decrease of their specific surface area.

Acknowledgements

References

[1] C. Liu, Y.Y. Fan, M. Liu, H.T. Cong, H.M. Cheng, and M. S. Dresselhaus. Hydrogen storage in single-walled carbon nanotubes at room temperature. Science, 1999, 286: 1127-1129.

[2] P.X. Hou, S.T. Xu, Z. Ying, Q.H. Yang, C. Liu, H.M. Cheng. Hydrogen adsorption / desorption behavior of multi-walled carbon nanotubes with different diameters. Carbon, 2003, 41: 2471–2476.

[3] K.L. Lu, R.M. Lago, Y.K. Chen, M.L.H. Green, P.J.F. Harris, S.C. Tsang. Mechanical damage of carbon nanotubes by ultrasound. Carbon, 1996, 34: 814–816.

[4] J. D. Teran, D.M. Nevskaia, J.L.G. Fierro, A.J.L. Peinado, A. Jerez. Study of chemical activation process of a lignocellulosic material with KOH by XPS and XRD.

Microporous and Mesoporous Materials, 2003, 60: 173–181.

[5] T. Yang, A. C. Lua. Characteristics of activated carbons prepared from pistachio-nut shells by potassium hydroxide activation. Microporous and Mesoporous

Materials, 2003, 63: 113–124.

[6] Q. Jiang, M.Z. Qu, B.L. Zhang, Z.L. Yu. Preparation of activated carbon nanotubes. Carbon, 2002, 40: 2743–2745.

[7] F. Liu, X.B. Zhang, J.P. Cheng , J.P. Tu , F.Z. Kong , W.Z. Huang, C.P. Chen. Preparation of short carbon nanotubes by mechanical ball milling and their hydrogen adsorption behavior. Carbon , 2003, 41: 2527–2532.

[8] K. Awasthi, R. Kamalakaran, A.K. Singh, O.N. Srivastava. Ball-milled carbon and

hydrogen storage. International Journal of Hydrogen Energy, 2002, 27: 425–432.

[9] N. Pierard, A. Fonseca, Z. Konya, I. Willems, G. Van Tendeloo, J.B. Nagy. Production of short carbon nanotubes with open tips by ball milling. Chemical physics letters, 2001, 335:1-8.

[10] Y.Y. Fan, F. Li, H.M. Cheng, G. Su, Y.D. Yu, Z.H. Shen. Preparation, morphology, and microstructure of diameter-controllable vapor-grown carbon nanofibers. Journal of Materials Research. 1998, 13: 2342–6.

[11] J. Choma, M. Jaroniec. A model-independent analysis of nitrogen adsorption isotherms on oxidized active carbon. Colloids and surfaces A. 2001, 189:103-111.